Role of the Added Ni in Hydrogen-Storage Reactions of MgH$_2$-Zn(BH$_4$)$_2$-Tm (Ni, Ti, or Fe) Alloys

Hye Ryoung PARK [1], Young Jun KWAK [2], Myoung Youp SONG [2] *

[1] *School of Chemical Engineering, Chonnam National University, 77 Yongbong-ro Buk-gu Gwangju, 61186, Republic of Korea*
[2] *Division of Advanced Materials Engineering, Hydrogen & Fuel Cell Research Center, Engineering Research Institute, Chonbuk National University, 567 Baekje-daero Deokjin-gu Jeonju, 54896, Republic of Korea*

In the present work, Zn(BH$_4$)$_2$, Ni, Ti, and/or Fe were doped to MgH$_2$ to improve the hydrogen absorption and release features. Samples with compositions of 95 w/o MgH$_2$ + 2.5 w/o Zn(BH$_4$)$_2$ + 2.5 w/o Ni (named MZN), 90 w/o MgH$_2$ + 5 w/o Zn(BH$_4$)$_2$ + 2.5 w/o Ni + 2.5 w/o Ti (named MZNT), and 90 w/o MgH$_2$ + 1.67 w/o Zn(BH$_4$)$_2$ + 5 w/o Ni + 1.67 w/o Ti + 1.67 w/o Fe (named MZNTF) were prepared by grinding in a planetary ball mill in a hydrogen atmosphere. The percentages of the additives were less than 10 w/o to increase hydrogen absorbing and releasing rates without a major sacrifice of the hydrogen-storage capacity. The hydrogen absorption and release features of the prepared samples were examined and in particular, the role of the added Ni in hydrogen-storage reactions of these alloys was studied. MZNTF had the effective hydrogen storage capacity (the quantity of hydrogen absorbed for 60 min) of near 5 w/o (4.98 w/o) at the third cycle (NC = 3). MZNTF had the highest initial releasing rate and the largest quantity of hydrogen released for 60 min, Q$_d$ (60 min), at 593 K under 1.0 bar hydrogen at the first cycle, followed in a descending order by MZNT and MZN. Ni formed Mg$_2$Ni by a reaction with Mg after hydrogen absorption-release cycling. Mg$_2$Ni and Mg are known to absorb and release hydrogen under similar temperature and hydrogen pressure conditions and Mg$_2$Ni is known to have higher hydrogen absorption and release rates than Mg. The formed Mg$_2$Ni phase is believed to contribute more strongly to the increases of the initial releasing rates and the Q$_d$ (60 min) by its hydride releasing hydrogen and slightly possibly providing paths for the hydrogen released from neighboring MgH$_2$, compared with the Zn formed after cycling and the TiH$_{1.924}$ formed after milling in hydrogen and remaining un-decomposed during cycling.

Keywords: hydrogen absorbing materials, mechanical milling, microstructure, role of Ni, MgH$_2$-based alloy.

1. INTRODUCTION

Magnesium hydride (MgH$_2$) has a certain number of advantages compared with the other two hydrides: the magnesium (Mg) exists in abundance, its price is less elevated, and Mg is light. However, Mg has the following two important weaknesses regarding the potential applications: MgH$_2$ releases hydrogen at relatively high temperature and its formation and decomposition rates are low.

The complex metal hydride zinc borohydride (Zn(BH$_4$)$_2$), one of the metal borohydrides, has attracted the interest of numerous researchers due to its high hydrogen density (8.4 w/o) [1] and its low decomposition temperature (323 – 393 K). Nakagawa et al. [1] synthesized Zn(BH$_4$)$_2$ by grinding zinc chloride (ZnCl$_2$) and sodium borohydride (NaBH$_4$) together. The preparation of the Zn(BH$_4$)$_2$ was accompanied by the formation of sodium chloride (NaCl). Nakamori et al. [2, 3] prepared the metal borohydrides M(BH$_4$)$_n$ (M = Ca, Sc, Ti, V, Cr, Mn, Zn (fourth period in periodic table), and Al; n = 2 – 4) using a mechanical grinding process. They reported that the hydrogen desorption temperature of the M(BH$_4$)$_n$ decreases as the Pauling electronegativity of the M increases.

In order to improve the hydrogen sorption properties of Mg, Ni [4 – 6], Ti [7, 8], and Ti and/or Ni [9] were added. Orimo et al. [6] synthesized the alloys Mg-x a/o Ni (x = 33, 38, 43, and 50) with different nanometer-scale structures by mechanically grinding the magnesium nickel (Mg$_2$Ni) mixed with various amounts of nickel (Ni). As the Ni content increased, the total hydrogen content increased from 1.7 w/o to 2.2 w/o and the hydrogen releasing temperature decreased from 440 K to 373 K. Lu et al. [9] synthesized core-shell structured binary Mg-Ti and ternary Mg-Ti-Ni composites using an arc plasma method followed by electroless plating in solutions. They reported that the hydrogenated composites with core–shell structures containing MgH$_2$ core and Ti or Mg-Ni hydrides shells were observed and the co-effect of TiH$_2$ and Mg$_2$Ni mainly improved the hydrogen sorption properties of Mg.

Srinivasan et al. [10] prepared zinc borohydride, Zn(BH$_4$)$_2$, by solid-state mechanochemical process. Various catalysts such as TiCl$_3$, TiF$_3$, nano Ni, nano Fe, Ti, nano Ti, and Zn were added to the borohydride to lower the decomposition temperature in the range of 323 – 373 K without significantly decreasing the hydrogen storage capacity of the sample. They reported that among the different catalysts, and 1.5 m/o nano Ni – added sample had the optimum behavior in terms of fast kinetics and decreasing the melting and decomposition temperature of Zn(BH$_4$)$_2$ [11].

---
* Corresponding author. Tel.: +82-63-270-2379; fax: +82-63-270-2386.
E-mail address: *songmy@jbnu.ac.kr* (M.Y. Song)

Zn(BH$_4$)$_2$, Ni, Ti, and/or Fe were picked as the dopants to promote the hydrogen absorbing and releasing rates of magnesium in this work.

In the present work, Zn(BH$_4$)$_2$, Ni, Ti, and/or Fe were doped to MgH$_2$ to improve the hydrogen absorbing and releasing features. Samples with compositions of 95 w/o MgH$_2$ + 2.5 w/o Zn(BH$_4$)$_2$ + 2.5 w/o Ni, 90 w/o MgH$_2$ + 5 w/o Zn(BH$_4$)$_2$ + 2.5 w/o Ni + 2.5 w/o Ti, and 90 w/o MgH$_2$ + 1.67 w/o Zn(BH$_4$)$_2$ + 5 w/o Ni + 1.67 w/o Ti + 1.67 w/o Fe were prepared by grinding in a planetary ball mill in a hydrogen atmosphere. The percentages of the additives were less than 10 w/o to increase hydrogen absorbing and releasing rates without a major sacrifice of the hydrogen storage capacity. The hydrogen absorption and release features of the prepared samples were examined and in particular, the role of the added Ni in hydrogen-storage reactions of these alloys was investigated. The samples were designated MZN, MZNT, and MZNTF, respectively.

2. EXPERIMENTAL DETAILS

MgH$_2$ (Aldrich, hydrogen-storage grade), the Zn(BH$_4$)$_2$ prepared in the authors' former study [12], Ni (Alfa Aesar, average particle size 2.2 – 3.0 μm, 99.9 % (metals basis), C typically < 0.1 %), Ti (Aldrich, − 325 mesh, 99 % (metals basis)), and Fe (Alfa Aesar GmbH (Germany), Iron particle size < 10 μm, purity 99.9 %) were utilized as starting materials without further purification.

Grinding was carried out under a hydrogen pressure of approximately 12 bar at a rotational speed of 400 rpm for 2 h in a planetary ball mill (Planetary Mono Mill; Pulverisette 6, Fritsch), as explained in the authors' previous study [13]. Mixtures with planned compositions were mixed with balls whose weight was 45 times the sample weight (ball to powder ratio = 45/1). Sample handling was undertaken in a glove box filled with argon (Ar).

The quantities of hydrogen absorbed by and released from samples as reaction time advances were measured by a volumetric method under approximately constant hydrogen pressures, using a Sieverts' type hydrogen absorbing and releasing apparatus, as presented previously [14]. The Sieverts' type hydrogen absorbing and releasing apparatus consisted of two parts: a standard volume and a reactor. The part of the standard volume included a reservoir with known volume linked to a Bourdon gauge M$_2$ which enabled the measurement of pressure in a range of 0 – 14 bar. The part of the reactor included a reactor and a Bourdon gauge M$_1$, identical with M$_2$, which was connected to the reactor by a capillary tube (internal diameter: about 4 mm). Hydrogen pressures were maintained nearly constant by dosing an appropriate amount of hydrogen from the standard volume to the reactor during hydriding reaction and by removing an appropriate amount of hydrogen from the reactor to the standard volume during dehydriding reaction. The quantity of hydrogen absorbed by or released from the samples as a function of time was calculated from the variation in the hydrogen pressure in the known standard volume.

Microstructures were observed by a scanning electron microscope (SEM, JEOL JSM-5900) at diverse magnifications for the samples ground in a hydrogen atmosphere and for those dehydrogenated after hydrogen absorption-release cycling. X-ray diffraction (XRD) patterns for the samples dehydrogenated after hydrogen absorption-release cycling were obtained using a powder diffractometer (Rigaku D/MAX 2500) with Cu Kα radiation (diffraction angle range 10 – 80°, scan speed 4°/min).

3. RESULTS AND DISCUSSION

The absorbed hydrogen quantity, Q$_a$, was defined as the percentage of absorbed hydrogen (w/o hydrogen) with respect to the sample weight. The released hydrogen quantity, Q$_d$, was also defined as the percentage of released hydrogen (w/o hydrogen) with respect to the sample weight. Before measuring Q$_a$ as a function of time t at the number of cycles, NC, of one (NC = 1), the prepared sample was heated to 623 K and hydrogen was released in vacuum for 1 h. To measure Q$_a$ versus t curves from NC = 2, the sample was heated to 623 K and hydrogen was released in vacuum for 1 h, after measuring the Q$_d$ versus t curve of the previous cycle.

Fig. 1 shows the Q$_a$ versus t curves at 593 K under 12 bar hydrogen for MZN, MZNT, and MZNTF at NC = 1.
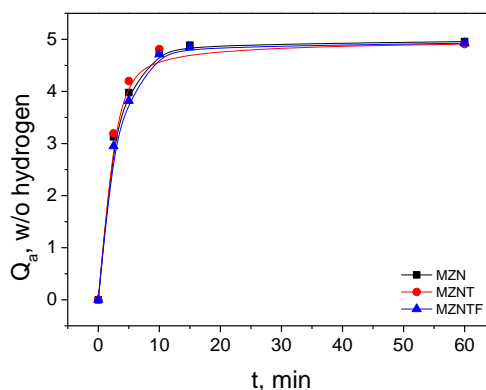

Fig. 1. Q$_a$ versus t curves at 593K under 12 bar hydrogen at NC = 1 for MZN, MZNT, and MZNTF

All the samples have quite high initial absorbing rates and quite large quantities of hydrogen absorbed after 60 min, Q$_a$ (60 min), showing that the addition of Zn(BH$_4$)$_2$, Ni, Ti, and/or Fe by milling in a hydrogen atmosphere increases the initial absorbing rate and the Q$_a$ (60 min). MZNT has the highest initial absorbing rate, followed in a descending order by MZN and MZNTF. They have very similar Q$_a$ (60 min). MZNTF absorbs 2.95 w/o hydrogen for 2.5 min, 3.82 w/o hydrogen for 5 min, 4.71 w/o hydrogen for 10 min, and 4.93 w/o hydrogen for 60 min. We define an effective hydrogen storage capacity as the quantity of hydrogen absorbed for 60 min. MZNTF has the effective hydrogen storage capacity of 4.93 w/o at NC = 1. Table 1 shows the changes in the Q$_a$ with the time t at 593 K under 12 bar hydrogen at NC = 1 for MZN, MZNT, and MZNTF.

The Q$_a$ versus t curves at 593 K under 12 bar hydrogen from the start to 10 min for MZN, MZNT, and MZNTF at NC = 1 are shown in Fig. 2. MZNT has the largest quantity of hydrogen absorbed after 10 min, Q$_a$ (10 min), followed in a descending order by MZN and MZNTF, but they have very similar Q$_a$ (10 min). Fig. 3 shows the Q$_a$ versus t curves at 593 K under 12 bar hydrogen for activated MZN
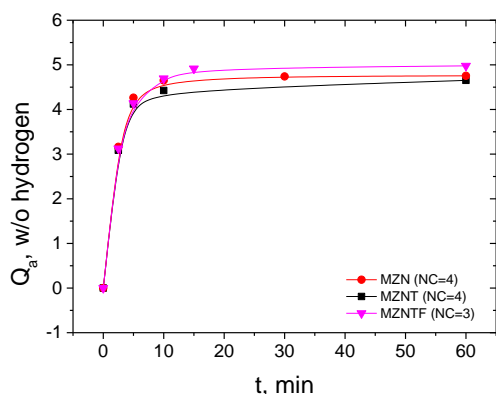
(NC = 4), MZNT (NC = 4), and MZNTF (NC = 3).

Table 1. Changes in the Q_a (w/o hydrogen) with the time t at 593 K under 12 bar hydrogen at the first cycle (NC = 1) for MZN, MZNT, and MZNTF

	2.5 min	5 min	10 min	60 min
MZN (MgH$_2$-2.5Zn(BH$_4$)$_2$-2.5Ni)	3.13	3.98	4.75	4.96
MZNT (MgH$_2$-5Zn(BH$_4$)$_2$-2.5Ni-2.5Ti)	3.20	4.20	4.82	4.91
MZNTF (MgH$_2$-1.67Zn(BH$_4$)$_2$-5Ni-1.67Ti-1.67Fe)	2.95	3.82	4.71	4.93
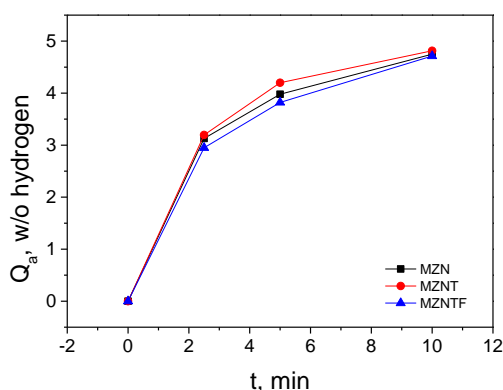
Fig. 2. Q_a versus t curves at 593 K under 12 bar hydrogen from the start to 10 min at NC = 1 for MZN, MZNT, and MZNTF

MZN has the highest initial absorbing rate, followed in a descending order by MZNTF and MZNT but they have very similar initial absorbing rates. MZNTF has the largest Q_a (60 min), followed in a descending order by MZN and MZNT. MZNTF (NC = 3) absorbs 3.12 w/o hydrogen for 2.5 min, 4.14 w/o hydrogen for 5 min, 4.70 w/o hydrogen for 10 min, and 4.98 w/o hydrogen for 60 min. MZNTF has the effective hydrogen storage capacity of 4.98 w/o at NC = 3. Table 2 shows the changes in the Q_a with the time t at 593 K under 12 bar hydrogen at NC = 3 or 4 for activated MZN, MZNT, and MZNTF.

Fig. 3. Q_a versus t curves at 593 K under 12 bar hydrogen for activated MZN (NC = 4), MZNT (NC = 4), and MZNTF (NC = 3)

All the samples have quite high initial releasing rates and quite large quantities of hydrogen released after 60 min, Q_d (60 min), showing that the addition of Zn(BH$_4$)$_2$, Ni, Ti, and/or Fe by milling in a hydrogen

atmosphere increases the initial releasing rate and the Q_d (60 min).

Table 2. Changes in the Q_a (w/o hydrogen) with the time t at 593 K under 12 bar hydrogen for activated MZN (NC = 4), MZNT (NC = 4), and MZNTF (NC = 3)

	2.5 min	5 min	10 min	60 min
MZN (NC = 4)	3.16	4.27	4.65	4.75
MZNT (NC = 4)	3.09	4.12	4.42	4.65
MZNTF (NC = 3)	3.12	4.14	4.70	4.98

The Q_d versus t curves at 593 K under 1.0 bar hydrogen at NC = 1 for MZN, MZNT, and MZNTF are shown in Fig. 4.
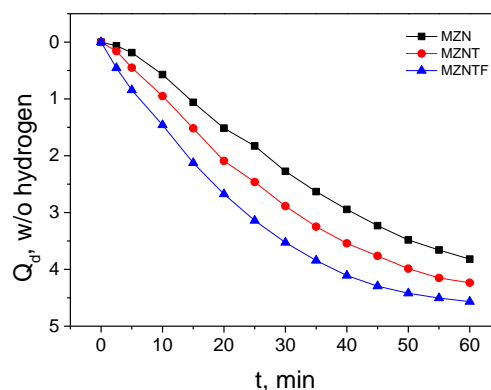
Fig. 4. Q_d versus t curves at 593 K under 1.0 bar hydrogen at NC = 1 for MZN, MZNT, and MZNTF

MZNTF has the highest initial releasing rate, followed in a descending order by MZNT and MZN. MZNTF releases 0.46 w/o hydrogen for 2.5 min, 0.84 w/o hydrogen for 5 min, 1.46 w/o hydrogen for 10 min, 2.68 w/o hydrogen for 20 min, and 4.57 w/o hydrogen for 60 min. Table 3 shows the changes in the Q_d with the time t at 593 K in 1.0 bar hydrogen at NC = 1 for MZN, MZNT, and MZNTF.

Table 3. Changes in the Q_d (w/o hydrogen) with the time t at 593 K under 1.0 bar hydrogen at the first cycle (NC = 1) for MZN, MZNT, and MZNTF

|	2.5 min	5 min	10 min	20 min	60 min
MZN	0.07	0.18	0.57	1.52	3.82
MZNT	0.16	0.45	0.95	2.09	4.24
MZNTF	0.46	0.84	1.46	2.68	4.57

Fig. 5 presents the SEM micrographs of MZN, MZNT, and MZNTF after milling in hydrogen. For all the samples, the particle sizes are not homogeneous: some particles are quite large and some particles are fine. Particles are irregular in shape. The particle sizes of three samples are similar, but MZN has the smallest particle size, followed in order by MZNTF and MZNT.

The XRD pattern of MZNTF after milling in hydrogen is shown in Fig. 6. The sample contains β-MgH$_2$, γ-MgH$_2$, Ni, TiH$_{1.924}$, Fe, and MgO. The XRD pattern of MZNTF dehydrogenated at 593 K under 1.0 bar hydrogen and then in vacuum at the 3rd hydrogen absorption–release cycle is shown in Fig. 7. The sample contains Mg and small amounts of β-MgH$_2$, MgO, Mg$_2$Ni, TiH$_{1.924}$, and Fe. This indicates that Ni formed Mg$_2$Ni by a reaction with Mg
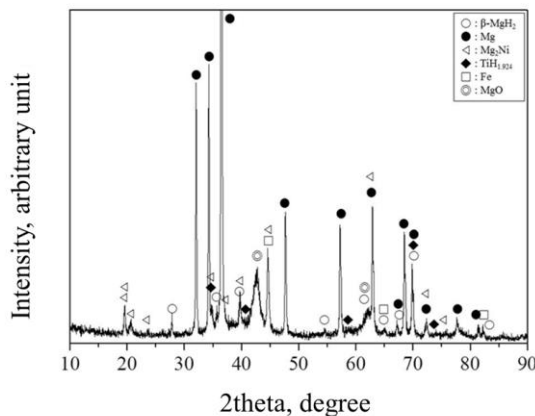
after hydrogen absorption-release cycling, and $TiH_{1.924}$ formed by the reaction of Ti with hydrogen during grinding in hydrogen is undecomposed even after hydrogen release reaction at 593 K under 1.0 bar hydrogen.
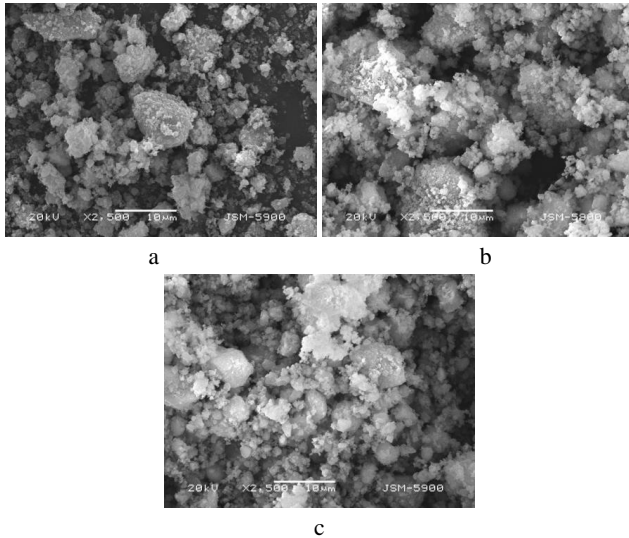
Fig. 5. SEM micrographs: a – MZN; b – MZNT; c – MZNTF after milling in hydrogen
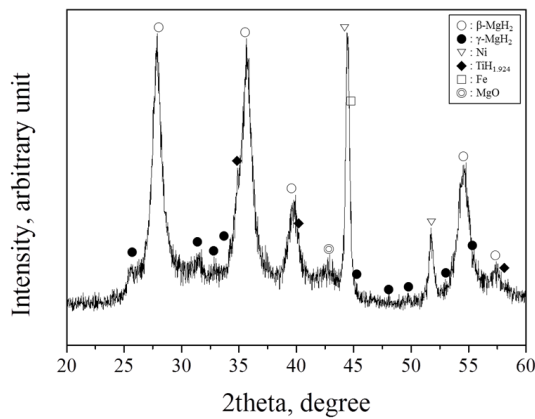
Fig. 6. XRD pattern MZNTF after milling in hydrogen

Fig. 7. XRD pattern of MZNTF dehydrogenated at 593 K under 1.0 bar hydrogen and then in vacuum at the 3rd hydrogen absorption-release cycle

The grinding in hydrogen of MgH_2 with $Zn(BH_4)_2$, Ni, and/or Ti is believed to create defects on the surface of and in the inside of the Mg particles, induce lattice strain, and make cracks. The propagation of cracks then decreases the particle sizes. The creation of defects, which can act as active sites for nucleation, facilitates nucleation. Making cracks and clean surfaces increases the reactivity of particles with hydrogen. Decreasing particle sizes shortens the diffusion distances of hydrogen atoms [15–19]. The induced lattice strain, which is revealed by the peak broadening and the increase in the backgrounds in XRD patterns, is thought to be released by hydrogen absorption-release cycling. The peak broadening got smaller and the backgrounds of XRD patterns after hydrogen absorption-release cycling were much lower, as compared with those in the XRD patterns of the as-milled samples [20].

Nakagawa et al. [1] reported that $Zn(BH_4)_2$ releases hydrogen with toxic diborane (B_2H_6), after melting with increasing temperature. The XRD pattern of $Zn(BH_4)_2 + MgH_2$, in which the mole ratio of $Zn(BH_4)_2$ to MgH_2 was 1 : 1, after heated up to 643 K showed that the sample contained NaCl, Zn, and MgH_2 [20]. For the measurements of hydrogen absorption and release properties, the sample was heated to 673 K and gases were released by pumping with a vacuum pump. It is thought that during this time in MZNTF, NaCl, $TiH_{1.924}$, and Fe remain un-reacted, and Zn, B_2H_6, Mg_2Ni, Mg, and H_2 are produced. During the subsequent hydrogen absorption-release cycling of the MZNTF sample, Zn, NaCl, and $TiH_{1.924}$, and Fe also remain un-reacted. Thus, during the subsequent hydrogen absorption-release cycling of the MZNTF sample, Mg and Mg_2Ni absorb and release hydrogen.

Fig. 1 shows that MZN, MZNT, and MZNTF have slightly different initial absorbing rates and very similar Q_a (60 min) at 593 K under 12 bar hydrogen at NC = 1. Fig. 3 shows that activated MZN, MZNT, and MZNTF have slightly different initial absorbing rates and MZNTF has the largest Q_a (60 min) at 593 K under 12 bar hydrogen. Fig. 4 shows that at 593 K in 1.0 bar hydrogen at NC = 1, the samples with a larger amount of additives (MZNTF and MZNT) have a higher initial releasing rate and a larger Q_d (60 min) than the sample with a smaller amount of additives (MZN). Fig. 4 also shows that at 593 K in 1.0 bar hydrogen at NC = 1, MZNTF has the highest initial releasing rate and Q_d (60 min), followed in a descending order by MZNT and MZN. This is considered to be resulted from the point that MZNTF has the largest content of the Mg_2Ni phase, followed in a descending order by MZNT and MZN.

Song et al. [21] reported that the rate-controlling steps of the hydrogen release reaction of Mg_2Ni hydride were the Knudsen flow and bulk flow of the hydrogen molecules through pores, interparticle channels or cracks. For the hydrogen release reaction at 575–615 K and 0.52–2.6 bar H_2 of an activated, mechanically alloyed mixture of 90 wt.% Mg + 10 w/o Ni, the rate-controlling steps were analyzed as both the bulk and Knudsen flows in the ranges of weight percentage of released hydrogen (H_d) higher than $0.5 < H_d \leq 0.1$. The hydrogen release rate was considered controlled mainly by the Knudsen flow as the ranges of weight percentage of desorbed hydrogen become higher [22]. The contraction due to the relatively rapid hydrogen release of Mg_2NiH_4 in the samples is believed to provide

paths for the hydrogen released from neighboring MgH_2, facilitating the hydrogen release of MgH_2.

Mg_2Ni and Mg are known to absorb and release hydrogen under similar temperature and hydrogen pressure conditions [23, 24]. The equilibrium plateau pressures at 593 K are 2.87 bar for $Mg-H_2$ system [25] and 4.99 bar for Mg_2Ni-H_2 system [26]. Mg_2Ni is known to have higher absorbing and releasing rates than Mg [23, 24]. The formed Mg_2Ni phase is believed to contribute more strongly to the increases of the initial releasing rates and the Q_d (60 min) by its hydride releasing hydrogen and slightly possibly providing paths for the hydrogen released from neighboring MgH_2, compared with the Zn formed after cycling and the $TiH_{1.924}$ formed after milling in hydrogen and remaining un-decomposed during cycling.

Fig. 5 shows that MZNTF has the largest particles. However, MZNTF has the highest initial releasing rate and the largest Q_d (60 min), indicating that the largest content of Ni in this sample plays an important role in the hydrogen release reaction.

The $TiH_{1.924}$ formed during grinding in hydrogen remains undecomposed even after hydrogen release reaction in vacuum. MZNT with a larger content of $TiH_{1.924}$ has lower initial releasing rate and smaller Q_d (60 min) than MZNTF with a smaller content of $TiH_{1.924}$. This shows that $TiH_{1.924}$ plays a role less importantly than Mg_2Ni in the hydrogen release reaction.

Table 4 shows the changes in the Q_a (w/o hydrogen) with the time t at 593 K under 12 bar hydrogen at NC = 1 for pure MgH_2 [27] and milled MgH_2 [28]. The milled MgH_2 sample was prepared by milling in a planetary ball mill (Planetary Mono Mill; Pulverisette 6, Fritsch) at a disc revolution speed of 250 rpm for 6 h. The pure MgH_2 absorbs hydrogen very slowly, with Q_a (60 min) of 0.04 w/o hydrogen. The milled MgH_2 absorbs very rapidly, with Q_a (60 min) of 7.11 w/o hydrogen.

Table 4. Changes in the Q_a (w/o hydrogen) with the time t at 593 K under 12 bar hydrogen at NC = 1 for pure MgH_2 and milled MgH_2

	2.5 min	5 min	10 min	60 min
pure MgH_2	0	–	–	0.04
milled MgH_2	3.92	5.44	6.85	7.11

Table 5 shows the changes in the Q_d (w/o hydrogen) with the time t at 593 K under 1.0 bar hydrogen at NC = 1 for pure MgH_2 [27] and milled MgH_2 [28]. The pure MgH_2 absorbs does not release hydrogen. The milled MgH_2 releases slowly, releasing 0.46 w/o hydrgen for 30 min and 2.01 w/o hydrgen for 60 min.

Table 5. Changes in the Q_d (w/o hydrogen) with the time t at 593 K under 1.0 bar hydrogen at NC = 1 for pure MgH_2 and milled MgH_2

	2.5 min	10 min	30 min	60 min
pure MgH_2	0	0	0	0
milled MgH_2	0	0	0.46	2.01

The MZN, MZNT, and MZNTF samples have lower initial absorbing rates and smaller H_a (60 min) than the milled MgH_2. However, they have higher releasing rates and larger H_d (60 min) than the milled MgH_2.

4. CONCLUSIONS

Samples MgH_2-2.5Zn(BH$_4$)$_2$-2.5Ni (MZN), MgH_2-5Zn(BH$_4$)$_2$-2.5Ni-2.5Ti (MZNT), and MgH_2-1.67Zn(BH$_4$)$_2$-5Ni-1.67Ti-1.67Fe (MZNTF) were prepared by grinding in a planetary ball mill in a hydrogen atmosphere. The activated MZN, MZNT, and MZNTF have slightly different initial absorbing rates and MZNTF has the largest Q_a (60 min). MZNTF had the highest initial releasing rate and the largest Q_d (60 min) at 593 K under 1.0 bar hydrogen at the first cycle, followed in a descending order by MZNT and MZN. Ni formed Mg_2Ni by a reaction with Mg after hydrogen absorption-release cycling. Mg_2Ni and Mg are known to absorb and release hydrogen under similar temperature and hydrogen pressure conditions and Mg_2Ni is known to have higher absorbing and releasing rates than Mg. The formed Mg_2Ni phase is believed to contribute more strongly to the increases of the initial releasing rates and the Q_d (60 min) by its hydride releasing hydrogen and slightly possibly providing paths for the hydrogen released from neighboring MgH_2, compared with the Zn formed after cycling and the $TiH_{1.924}$ formed after milling in hydrogen and remaining un-decomposed during cycling.

REFERENCES

1. **Nakagawa, T., Ichikawa, T., Kojima, Y., Fujii, H.** Gas Emission Properties of the MgH_x-Zn(BH$_4$)$_2$ Systems *Materials Transactions* 48 2007: pp. 556–559. https://doi.org/10.2320/matertrans.48.556

2. **Nakamori, Y., Li, H.-W., Kikuchi, K., Aoki, M., Miwa, K., Towata, S., Orimo, S.** Thermodynamical Stabilities of Metal-Borohydrides *Journal of Alloys Compounds* 446–447 2007: pp. 296–300. https://doi.org/10.1016/j.jallcom.2007.03.144

3. **Nakamori, Y., Li, H.W., Matsuo, M., Miwa, K., Towata, S., Orimo, S.** Development of Metal Borohydrides for Hydrogen Storage *Journal of Physics and Chemistry of Solids* 69 2008: pp. 2292–2296. https://doi.org/10.1016/j.jpcs.2008.04.017

4. **Révész, Á., Gajdics, M., Spassov, T.** Microstructural Evolution of Ball-Milled Mg–Ni Powder during Hydrogen Sorption *International Journal of Hydrogen Energy* 38 2013: pp. 8342–8349. https://doi.org/10.1016/j.ijhydene.2013.04.128

5. **Zou, J., Long, S., Chen, X., Zeng, X., Ding, W.** Preparation and Hydrogen Sorption Properties of a Ni Decorated Mg Based Mg@Ni Nano-Composite *International Journal of Hydrogen Energy* 40 2015: pp. 1820–1828. https://doi.org/10.1016/j.ijhydene.2014.11.113

6. **Orimo, S., Ikeda, K. Fujii, H., Fujikawa, Y., Kitano, Y., Yamamoto, K.** Structural and Hydriding Properties of the Mg-Ni-H System with Nano- and/or Amorphous Structures *Acta Materilia* 45 1997: pp. 2271–2278. https://doi.org/10.1016/S1359-6454(96)00357-6

7. **Calizzi, M., Chericoni, D., Jepsen, L.H., Jensen, T.R., Pasquini, L.** Mg–Ti Nanoparticles with Superior Kinetics

for Hydrogen Storage *International Journal of Hydrogen Energy* 41 2016: pp. 14447–14454.
https://doi.org/10.1016/j.ijhydene.2016.03.071

8. **Phetsinorath, S., Zou, J.X., Zeng, X.Q., Sun, H.Q., Ding, W.J.** Preparation and Hydrogen Storage Properties of Ultrafine Pure Mg and Mg–Ti Particles *Transactions of Nonferrous Metals Society of China* 22 2012: pp. 1849–1854.
https://doi.org/10.1016/S1003-6326(11)61396-4

9. **Lu, C., Zou, J., Shi, X., Zeng, X., Ding, W.** Synthesis and Hydrogen Storage Properties of Core–Shell Structured Binary Mg@Ti and Ternary Mg@Ti@Ni Composites *International Journal of Hydrogen Energy* 42 2017: pp. 2239–2247.
https://doi.org/10.1016/j.ijhydene.2016.10.088

10. **Srinivasan, S., Escobar, D., Goswami, Y., Stefanakos, E.** Effects of Catalysts Doping on the Thermal Decomposition Behavior of $Zn(BH_4)_2$ *International Journal of Hydrogen Energy* 33 2008: pp. 2268–2272.
https://doi.org/10.1016/j.ijhydene.2008.02.062

11. **Srinivasan, S., Escobar, D., Jurczyk, M., Goswami, Y., Stefanakos, E.** Nanocatalyst Doping of $Zn(BH_4)_2$ for On-Board Hydrogen Storage *Journal of Alloys and Compounds* 462 2008: pp. 294–302.
https://doi.org/10.1016/j.jallcom.2007.08.028

12. **Kwak, Y.J., Kwon, S.N., Lee, S.H., Park, I.W., Song, M.Y.** Synthesis of $Zn(BH_4)_2$ and Gas Absorption and Release Characteristics of $Zn(BH_4)_2$, Ni, or Ti-Added MgH_2 –Based Alloys *Korean Journal of Metals and Materials* 53 2015: pp. 500–505.
https://doi.org/10.3365/KJMM.2015.53.7.500

13. **Kwak, Y.J., Lee, S.H., Park, H.R., Song, M.Y.** Hydrogen-Storage Property Enhancement of Magnesium Hydride by Nickel Addition via Reactive Mechanical Grinding *Korean Journal of Metals and Materials* 51 2013: pp. 607–613.
https://doi.org/10.3365/KJMM.2013.51.8.607

14. **Song, M.Y., Baek, S.H., Bobet, J.L., Song, J., Hong, S.H.** Hydrogen Storage Properties of a Mg-Ni-Fe Mixture Prepared via Planetary Ball Milling in a H_2 Atmosphere *International Journal of Hydrogen Energy* 35 2010: pp. 10366–10272.
https://doi.org/10.1016/j.ijhydene.2010.07.161

15. **Hong, S.H., Song, M.Y.** Study on the Reactivity with Hydrogen of Planetary Ball Milled 90 wt% Mg+10 wt% MgH_2: Analyses of Reaction Rates with Hydrogen and Microstructure *Korean Journal of Metals and Materials* 54 2016: pp. 358–363.
https://doi.org/10.3365/KJMM.2016.54.5.358

16. **Hong, S.H., Song, M.Y.** Preparation of Mg-MgH_2 Flakes by Planetary Ball Milling with Stearic Acid and Their Hydrogen Storage Properties *Metals and Materials International* 22 2016: pp. 544–549.
https://doi.org/10.1007/s12540-016-5557-0

17. **Song, M.Y., Kwak, Y.J., Park, H.R.** Hydrogen Storage Characteristics of Metal Hydro-Borate and Transition Element-Added Magnesium Hydride *Korean Journal of Metals and Materials* 54 2016: pp. 503–509.
https://doi.org/10.3365/KJMM.2016.54.7.503

18. **Kwon, S.N., Park, H.R., Song, M.Y.** Hydrogen Storage and Release Properties of Transition Metal-Added Magnesium Hydride Alloy Fabricated by Grinding in a Hydrogen Atmosphere *Korean Journal of Metals and Materials* 54 2016: pp. 510–519.
https://doi.org/10.3365/KJMM.2016.54.7.510

19. **Park, H.R., Kwak, Y.J., Song, M.Y.** Increase in the Hydrogen-Sorption Rates and Hydrogen-Storage Capacity of MgH_2 by Adding a Small Proportion of $Zn(BH_4)_2$ *Korean Journal of Metals and Materials* 55 2017: pp. 656–662.
https://doi.org/10.3365/KJMM.2017.55.9.657

20. **Kwak, Y.J., Park, H.R., Song, M.Y.** Changes in Microstructure, Phases, and Hydrogen Storage Characteristics of Metal Hydro-Borate and Nickel-Added Magnesium Hydride with Hydrogen Absorption and Release Reactions *International Journal of Hydrogen Energy* 42 2017: pp. 1018–1026.
https://doi.org/10.1016/j.ijhydene.2016.10.097

21. **Song, M.Y., Darriet, B., Pezat, M., Lee, J.Y., Hagenmuller, P.** Dehydriding Kinetics in Mg_2Ni-H_2 System *Journal of the Less-Common Metals* 118 1986: pp. 235–248.
https://doi.org/10.1016/0022-5088(86)90173-6

22. **Song, M.Y., Manaud, J.P., Darriet, B.** Dehydriding Kinetics of a Mechanically-Alloyed Mixture Mg-10 wt.% Ni *Journal of Alloys and Compounds* 282 1999: pp. 243–247.
https://doi.org/10.1016/S0925-8388(98)00821-4

23. **Reilly, J.J., Wiswall, Jr.R.H.** The Reaction of Hydrogen with Alloys of Magnesium and Nickel and the Formation of Mg_2NiH_4 *Inorganic Chemistry* 7 1968: pp. 2254–2256.
https://doi.org/10.1021/ic50069a016

24. **Song, M.Y., Ivanov, E., Darriet, B., Pezat, M., Hagenmuller, P.** Hydriding and Dehydriding Characteristics of Mechanically Alloyed Mixtures Mg-x wt.% Ni (x=5, 10, 25 and 55) *Journal of the Less-Common Metals* 131 1987: pp. 71–79.
https://doi.org/10.1016/0022-5088(87)90502-9

25. **Song, M.Y., Kwak, Y.J.,** Comparison of the Hydrogen Release Properties of Zn(BH4)2-Added MgH2 Alloy and Zn(BH4)2 and Ni-Added MgH2 Alloy *Korean Journal of Metals and Materials* 56 2018: pp. 244–251.
https://doi.org/10.3365/KJMM.2018.56.3.244

26. **Song, M.Y., Park, H.R.** Pressure-Composition Isotherms in Mg_2Ni-H_2 System *Journal of Alloys and Compounds* 270 1998: pp. 164–167.
https://doi.org/10.1016/S0925-8388(98)00459-9

27. **Song, M.Y, Kwak, Y.J., Lee, S.H., Park, H.R.** Comparison of Hydrogen Storage Properties of Pure MgH_2 and Pure Mg *Korean Journal of Metals and Materials* 52 2014: pp. 689–693.
https://doi.org/10.3365/KJMM.2014.52.9.689

28. **Song, M.Y., Kwak, Y.J., Lee, S.H., Park, H.R.** Comparison of the Hydrogen Storage Properties of Pure Mg and Milled Pure Mg *Bulletin of Materials Science* 37 2014: pp. 831–835.
https://doi.org/10.1007/s12034-014-0013-6